A major purpose of the Technical Information Center is to provide the broadest dissemination possible of information contained in DOE's Research and Development Reports to business, industry, the academic community, and federal, state and local governments.

Although a small portion of this report is not reproducible, it is being made available to expedite the availability of information on the research discussed herein.

LA-UR -86-2130

CONF-860883--1

Los Alamos National Laboratory is operated by the University of California for the United States Department of Energy under contract W-7405-ENG-36.

LA-UR--86-2130

DE86 012403

TITLE: PLASMA SYNTHESIS AND CHARACTERIZATION OF ULTRAFINE SiC

AUTHOR(S): Gerald J. Vogt (MST-3) and David S. Phillips (MST-6)
Materials Science and Technology Division
Los Alamos National Laboratory, Los Alamos, NM 87545

Thomas N. Taylor (CHM-2)
Chemistry Division
Los Alamos National Laboratory, Los Alamos, NM 87545

SUBMITTED TO: Ceramic Powder Science and Technology Conference
American Ceramic Society
Boston, MA
August 3-6, 1986

DISCLAIMER

PLASMA SYNTHESIS AND CHARACTERIZATION OF ULTRAFINE SiC

G.J. Vogt and D.S. Phillips,
Materials Science and Technology Division

T.N. Taylor
Chemistry Division

Los Alamos National Laboratory
Los Alamos, New Mexico 87545

ABSTRACT

Ultrafine SiC powders have been prepared by gas phase synthesis from silane and methane in an argon thermal rf-plasma. Bulk properties of the powders were determined by elemental analysis, x-ray diffraction, helium pycnometry, and BET surface area measurements. The near-surface composition and structure of the particles were examined by x-ray photoelectron spectroscopy (XPS) and transmission electron microscopy (TEM). In addition to free silicon and carbon particles in the powders, free carbon and various silicon/carbon/oxygen species were found on the surface of the SiC particles. The presence of these surface species will dominate the powder surface chemistry, having important implications for powder processing and consolidation.

INTRODUCTION

Growing interest in ultrafine silicon carbide powders has arisen from the possible application of these powders to the preparation of high temperature structural ceramics. The physical and chemical properties of the powders will be dominant factors for the control of the microstructure and physical properties of the consolidated ceramic prepared by sintering

processes. Important properties [1] generally sought for successful consolidation include chemical stoichiometry and purity, small particle size with a narrow size distribution, equiaxed morphologies, and the absence of hard agglomerates. More fundamentally, the surface composition and chemistry of the plasma SiC powders will play a critical role in the formation of a satisfactory green body by dispersion processing and in the later sintering of the compact.

Numerous investigators [2] have studied the preparation of silicon carbide powder by thermal plasma chemical synthesis. The powders are typically spheroidal in shape with an ultrafine size (5-100 nm), consisting predominately of the beta-SiC phase (as seen by XRD analysis). Examination by TEM generally shows a significant fraction of agglomerates, which seem to be largely hard (sintered) in nature. Bulk chemical analysis of the powders shows that the powders can be prepared in a large variety of C/Si atomic ratios, ranging from silicon rich (<1.0) to carbon rich (>1.0). Although considerable effort is given to preparing powder with a C/Si ratio near 1.0 as determined by bulk analysis, the question still remains whether the particle surfaces contain any non-carbide silicon or carbon phases. Particle surface composition does not necessarily reflect that of the bulk. The presence of these non-carbide silicon or carbon species on the particle surfaces will strongly influence the powder surface chemistry and dispersibility.

The average surface composition and bonding of ultrafine SiC powders, prepared at Los Alamos by thermal rf-plasma synthesis,

have been characterized by x-ray photoelectron spectroscopy (XPS) and Auger electron spectroscopy (AES). The same powders have also been examined for surface and bulk phases of silicon and carbon by transmission electron microscopy (TEM). In this paper the results of surface chemical and microstructural studies will be discussed in light of their significance to colloidal processing and with specific suggestions on how the surface chemistry of the powders may be altered in synthesis and by post-synthesis treatment. The synergistic effort of plasma synthesis, surface analytical measurements, and powder colloidal characterization, we believe, is essential to the eventual understanding of the colloidal dispersion of plasma-prepared SiC and subsequent additive-free densification of the powder.

EXPERIMENTAL

Synthesis of Silicon Carbide

Silicon carbide powders were synthesized by the chemical reaction of silane and methane in the energetic tail flame from a thermal inductively-coupled argon plasma [3-5]. The reactor, shown schematically in Fig. 1, included an induction tube, designed at Los Alamos, with a 75-kW rf generator and a water-cooled stainless steel quenching chamber. The main argon stream to the rf plasma was tangentially injected at the top of the induction tube with a tail flame extending into the quenching chamber. A cold quench gas can be added to the system through an annular jet located between the induction tube and the quenching chamber. The reactant mixture was introduced into the tail flame through a water-cooled stainless steel probe, positioned along

the central axis of the plasma and its tail flame, as shown in Fig. 1. The point where the reactants enter the tail flame can be varied by raising or lowering the probe. The powders were swept out of the quenching chamber with the exhaust gases and collected on sintered metal filters or by cyclone separators.

Reaction conditions are summarized in Tables I and II. The induction plasma tube was operated at a frequency of 360 kHz and a typical plate power of 30 kW. The main plasma argon stream was fed into the reactor at a typical flow rate of 28-29 standard liters per minute (slpm) at STP with a chamber pressure near 600 torr. The argon quench flow was set between 3 and 12 slpm. Duration of the synthesis runs ranged from 1.5 to 4.3 hours without any observed restrictions for even longer run times. The increased yield for Run 40 over the other runs resulted from using absolute filters to collect the plasma powder rather than cyclone separators. Run 41 was a duplicate of Run 40 with special precaution taken to collect and store the powders in an inert atmosphere. The plasma powders were routinely characterized by elemental analysis, x-ray diffraction, multipoint BET measurements of their specific surface area, and by helium pycnometry for true densities.

Some characteristics of the plasma SiC powders are given in Table II. The total silicon utilization (fraction of silane converted to powder material) in the plasma reactor was well above 92% for Run 40. In this experiment with a run time of 1.5 hours, 82% of the powder was found in the downstream powder collector and the remaining 18% in the quenching chamber. In all synthesis

runs shown in Table II, excess methane was used with silane to generate silicon carbide. Despite this excess methane, silicon-rich powders can be produced as seen in Run 24. Powders 24, 40, and 41 were chosen as representative silicon-rich and carbon-rich samples for further examination by XPS, AES, and TEM.

Surface Characterization

We have used XPS to determine the average surface composition and chemical bonding of these ultrafine silicon carbide powders. The energy spectrum of photoelectrons produced from a powder material by Mg-K_α radiation ($h\nu$ = 1253.6 eV) was measured with a hemispherical analyzer which had been calibrated using atomically clean Ag and Au standards. For Mg-K_α radiation, the kinetic energy of photoelectrons from Si, C, and O is greater than 700 eV and, thus, the measurement of these species probes ~2.0 nm into the individual powder particles [6]. (This analysis examines an outer shell with a thickness of approximately 50 per cent of the volume of a 20 nm diameter sphere.) We have also employed AES to make complementary measurements of powder composition.

The powders under study had either been stored in air for more than six months or under glovebox conditions at <2 ppm of oxygen. Air-stored samples were pressed onto an indium support in a continuous layer using a double-sided compaction technique that revealed only virgin powder for analysis. In order to simplify this procedure, the glovebox-stored powders were applied to the indium in situ using a clean glass slide. Air-stored powder mounted using these two compaction techniques showed no

measurable XPS or AES differences. The powder/support was mounted on a transfer rod and introduced into the vacuum chamber for analysis at pressures $\leq 10^{-8}$ Torr. Samples that had been stored and compacted on indium under glovebox conditions were kept in containers purged with dry N_2 during the mounting procedure.

TEM Characterization.

The powder samples described here were prepared for examination in the transmission electron microscope (TEM) by dipping holey carbon films into dilute dispersions prepared by sonicating the powder in methanol. Other organic suspensions were studied but rejected either because of excessive agglomeration during drying (butanol) or because they left heavy residues on the particle surfaces (carbon tetrachloride). These samples were then examined in conventional TEM at 120 kV. Particles supported by homogeneous patches of carbon support film were suitable for determination of particle sizes and shapes and for estimation of relative levels of agglomeration among powders. Portions of large agglomerates suspended above holes in the film were used for qualitative phase analyses using electron diffraction and for high resolution imaging.

RESULTS

Powder Surface Chemistry

The XPS and AES measurements revealed only silicon, carbon, and oxygen containing species on the powders. As indicated in Table III for the powder runs 40, 41, and 24 examined by XPS in

this study, the air-stored powders had larger atom fractions of C and O than did those stored under glovebox conditions. The oxygen atom fraction is at least two times larger for the powders stored in air. Adsorption of C and O containing contaminants during air storage acts to cover the Si and hence reduce its atom fraction at the surface.

Measurement of the C(1s) peak for the air-stored powders 40 and 24 gives the XPS spectra (intensity versus binding energy, BE) shown in Fig. 2. These data show a pronounced doublet from both powders with peak energies (282.8 $\pm$ 0.1 and 284.1 $\pm$ 0.1 eV BE) near those associated with carbide bonding and C-C or graphitic bonding, respectively [7-9]. The high binding energy region within 3 eV of the C-C peak allows for the existence of C-H and C-OH species on these surfaces [10,11]. Only a smooth background intensity is found above ~287.0 eV BE and consequently we conclude that there is no significant C-O bonding on the powders. This agrees with recent nmr measurements on the powders at Los Alamos [12]. The comparable glovebox-stored powders (41 and 24) show very similar C(1s) peaks where the C-C to carbide intensities vary no more than 10 per cent from the air-stored samples.

A second set of XPS data for the Si(2p) peak from the air-stored powders (40 and 24), shown in Fig. 3, gives peak positions at 100.4 $\pm$ 0.1 eV BE. They agree well with the Si(2p) values of 100.20 eV BE measured from cleaved and/or sputtered SiC [8] and 100.4 eV BE measured from sputtered SiC(000$\bar{1}$) and SiC(0001) [9]. Note, however, that the peak width (FWHM) for powder 40 is

0.30 eV smaller than that for powder 24, indicating better state definition. We have consequently taken the Si(2p) peak from powder 40 as a reference spectrum most like that for pure SiC bonding. By subtracting this reference peak from that for powder 24, one can get a semiquantitative measure of the additional Si bonding states present in powder 24. Proper scaling and normalization gives the difference plot at the top of Fig. 3. Clearly, powder 24 contains additional Si(2p) spectral content both below and above the carbide peak position. Substantial difference peaks are observed near 99.3 and 101.4 eV BE. The former peak is near accepted values for elemental Si [8,13], while the latter is attributable to O-Si-C (101.0 to 102.0 eV BE) [8] and SiO_{2-x} species. There is no measurable evidence for SiO_2 at 103.4 eV BE [10,13]. The suboxides have been observed by XPS over the binding energy range from SiC to SiO_2 in studies of both chemisorbed [14] and thin (<1.0 nm) thermally grown oxide layers [15,16]. The parent Si(2p) peaks for the glovebox-stored powders are also located at 100.4 $\pm$ 0.1 eV BE. However, the higher binding energy difference peak found on air-stored powder 24 is much better developed than that for glovebox-storage; the Si(2p) FWHM increasing from 1.76 to 1.84 eV after air storage. The O(1s) peaks are found near 531.7 $\pm$ 0.1 eV BE (powder 40 and 41) and 531.9 $\pm$ 0.1 eV BE (powder 24), more than 0.5 eV BE below the value reported for stoichiometric SiO_2 [13] and consistent with our Si(2p) peak assignments.

Transmission Electron Microscopy

Cursory TEM examination under low resolution of the plasma SiC powders shows remarkable similarity between runs. A typical example is seen in Fig. 4 for powder 24. All powders showed similar distributions of primary particle sizes near 20 nm average diameter. These primary particles were arranged into a wide variety of agglomerate sizes and shapes extending up to 3 microns apparent diameter. Ring diffraction patterns from the silicon-rich powder 24 in Fig. 5 indicate a mixture of Si and beta-SiC particles. No evidence of either graphitic carbon or any of the alpha-SiC phases was detected by electron diffraction.

High resolution imaging of the SiC particles has, however, shown some striking distinctions among different powder runs (see Figs. 6 and 7). First, these images show that the primary 20 nm particles are basically single crystals of SiC, sometimes including twins and stacking faults. Second, both silicon-rich powder 24 and carbon-rich powder 40 contain apparent carbon inclusions. These inclusions are partly responsible for the large C/Si surface atom fraction ratios found in Table III. In the carbon-rich powders, such as lot 40, they are often sufficiently crystalline to be recognized by the 0.34 nm fringe periodicity of graphite (0001) planes, as seen in Fig. 7. Many of these carbon inclusions show hollow braid-like morphologies; the carbon inclusions labelled in Fig. 4 were identified on the basis of analogy with these particles. Finally, the primary SiC particles from carbon-rich runs (similar to runs 40 and 41) often show graphitic carbon coatings (identified from fringe

periodicity) of apparent unit-cell thicknesses. Such a coating is demonstrated in Fig. 7.

DISCUSSION

The XPS and TEM results demonstrate that powder 24 has bulk and surface components that are different from those found in the more SiC-like powders 40 and 41. Being silicon-rich, the agglomerates in powder 24 should exhibit a silicon/oxygen/carbon surface chemistry which is influenced by free silicon particles and unhindered by the protective carbon coating found typically on the carbon-rich powders. Preliminary work at Los Alamos in the area of colloidal processing has shown that these silicon-rich powders are much more effectively suspended using silicon oxide dispersion schemes than are the carbon-rich powders. This is undoubtedly tied to the above described differences in powder surface composition, where the silicon compound (O-Si-C and/or SiO_{2-x}) sites mimic the wet chemical behavior of pure silicon oxide surfaces [17]. These silica dispersion routes might be utilized for silicon carbide processing, if synthesis and post-synthesis chemical tailoring are employed to eliminate the carbon coating and produce monolayer thick silicon oxide on the more SiC-like powders, such as found in lots 40 and 41.

The presence of free carbon particles in the plasma powders is not remarkable, since the reactant gas streams for all syntheses were methane-rich (see Table II). It seems likely that a portion of the molecular fragments produced by dissociation of methane in the plasma later recombines to give methane and some higher hydrocarbon species (e.g., acetylene and ethylene), which

then crack at the particle surfaces during cooling to leave elemental carbon. It is possible that this cracking on the surfaces of the primary SiC particles occurs at relatively high temperatures to yield a truly crystalline product, while at lower temperatures amorphous carbon could form. It is also possible that the particle coatings are in fact similar to the free inclusions, since even amorphous carbons are thought to be ordered over ranges larger than three layers. Carbon coatings on silicon carbide particles may also be formed by the decomposition of SiC at the particle surface through sublimation of Si at high temperatures. This carbonizing or graphitization mechanism has been proposed [1] and studied [7,9] by other investigators. Since both cracking and graphitization mechanisms would occur at elevated temperatures, enhanced quenching of the plasma process may suppress the formation of the carbon coatings.

In the event that carbon coatings cannot be eliminated during synthesis, post-synthesis treatment of the powders may be an alternative for carbor removal. A simple method would be to heat treat the plasma powders at 1000-1200 K and under a pure hydrogen atmosphere. This type of post-synthesis treatment has proven quite successful in the removal of free carbon in plasma nickel powders [5]. As part of colloidal processing strategy, the hydrogen heat treatment could be performed to remove the carbon before dispersing the powder and preparing the green bodies. Subsequent atmospheric exposure of the treated powders at lower temperatures might conveniently produce the thin surface oxidation needed for successful dispersion. Alternately, after

dispersing the carbon-coated powder, using a carbon dispersion scheme, and forming a compact, the powder could be degraphitized in hydrogen immediately before sintering the compact, as an oxygen-free atmosphere will be needed in any case to prevent heavy oxidation of the ultrafine particles.

However the carbon coatings form, their implications for subsequent processing are quite important. Indeed, we have verified that their chemical characteristics differ substantially from those of oxidized silicon (silanol) species, making dispersion and wet casting processes more difficult. On the other hand, these coatings also protect the particles against oxidation, making them part of an attractive model system for studying the wet processing and sintering of covalent non-oxide ceramics.

ACKNOWLEDGMENTS

The authors gratefully acknowledge the advice and assistance of C.T. Campbell and M.T. Paffett at Los Alamos in the surface characterization of the powders. Helpful information was also obtained from J.T. Yates, Jr., (University of Pittsburgh, Pittsburgh, PA) and M. Hecht (Jet Propulsion Laboratory, Pasadena, CA).

This work was supported by the Office of Basic Energy Sciences of the Division of Materials Sciences of the U.S. Department of Energy and by the Institutional Supported Research and Development Program at the Los Alamos National Laboratory.

REFERENCES

1. Y. Suyama, R.M. Marra, J.S. Haggerty, and H.K. Bowen, "Synthesis of Ultrafine SiC Powders by Laser-Driven Gas Phase Reactions," Bull. Am. Ceram. Soc., 64(10), 1356-59 (1985).
2. G.J. Vogt and L.R. Newkirk, "Thermal Plasma Chemical Synthesis of Powders," Proceedings of the Symposium on High Temperature Materials Chemistry-III (The Electrochemical Society,Inc., Pennington, NJ), 164-176 (1986).
3. C.M. Hollabaugh, D.E. Hull, L.R. Newkirk, and J.J. Petrovic, "R.F.-Plasma System for the Production of Ultrafine, Ultrapure Silicon Carbide Powder," J. Mater. Sci., 16, 3190-94 (1983).
4. G.J. Vogt, C.M. Hollabaugh, D.E. Hull, L.R. Newkirk, and J.J. Petrovic, "Novel RF-Plasma System for the Synthesis of Ultrafine, Ultrapure SiC and Si_3N_4," Mat. Res. Sym. Proc., 30, 283-9 (1984).
5. G.J. Vogt, R.S. Vigil, L.R. Newkirk, and M. Trkula, "Synthesis of Ultrafine Ceramic and Metallic Powders in a Thermal Argon RF-Plasma," Seventh International Symposium on Plasma Chemistry, Eindhoven, 668-73 (1985).
6. M.P. Seah and W.A. Dench, "Quantitative Electron Spectroscopy of Surfaces: A Standard Data Base for Electron Inelastic Mean Free Paths in Solids," Surf. and Interface Anal., 1(1), 2-11 (1979).
7. K. Miyoshi and D.H. Buckley, "XPS, AES and Friction Studies of Single-Crystal Silicon Carbide," Appl. Surf. Sci., 10, 357-76 (1982).

8. K.L. Smith and K.M. Black, "Characterization of the Treated Surfaces of Silicon Alloyed Pyrolytic Carbon and SiC," J. Vac. Sci. Technol., A2(2), 744-7 (1984).

9. L. Muehlhoff, W.J. Choyke, M.J. Bozack, and J.T. Yates, Jr., "Comparative Electron Spectroscopy Studies of Surface Segregation on SiC(000$\bar{1}$) and SiC(0001)," submitted to J. Appl Phys.

10. C.D. Wagner, W.M. Riggs, L.E. Davis, and G.E. Muilenberg, Handbook of X-ray Photoelectron Spectroscopy (Physical Electronics Division, Perkin-Elmer Corp., Eden Prairie, MN, 1979).

11. R. Schlögl and H.P. Boehm, "Influence of Crystalline Perfection and Surface Species on the X-ray Photoelectron Spectra of Natural and Synthetic Graphite," Carbon, 21(4), 345-58 (1983).

12. Private communication with W.L. Earl, Los Alamos National Laboratory.

13. C.D. Wagner, H.A. Six, W.T. Jansen, and J.A. Taylor, "Auger and Photoelectron Line Energy Relationships in Aluminum-Oxygen and Silicon-Oxygen Compounds," J. Vac. Sci. Technol., 21(4), 933-44 (1982).

14. C.M. Garner, I. Lindau, C.Y. Su, P. Pianetta, and W.E. Spicer, "Electron-Spectroscopic Studies of the Early Stages of the Oxidation of Si," Phys. Rev. B, 19(8), 3944-56 (1979).

15. R. Flitsch and S.I. Raider, "Electron Mean Escape Depths from X-ray Photoelectron Spectra of Thermally Oxidized Silicon

Dioxide Films on Silicon," J. Vac. Sci. Technol., 12(1), 305-8 (1975).

16. A. Ishishizaka, S. Iwata, and Y. Kamigaki, "Si-SiO_2 Interface Characterization by ESCA," Surf. Sci., 84, 355-74 (1979).

17. R.K. Iler, "The Chemistry of Silica," (John Wiley & Sons, New York, 1979), 312-461.

Table I. Reaction Conditions

Run No.	Power (kW)	Plasma Argon (slpm)	Quench Argon (slpm)	Probe* Depth (cm)	Yield (g/hr)
24	28	27.1	12	9.8	45
27B	32	29.4	6.2	5.7	48
31	29	27.6	11	9.7	--
35D	29	27.6	11	15.9	23
40	30-31	29.8	11	15.9	79
41	30	29.8	3.7	15.9	--

*Probe depth is distance of probe tip below rf coil.

TABLE II. Reactant Flow Rates and Powder Properties

Run No.	SiH_4 (slpm)	CH_4 (slpm)	Reactant Gas C/Si (mol/mol)	Powder C/Si (mol/mol)	BET Surface Area (m^2/g)	BET Equivalent Diameter (nm)	Density (g/cm^3)
24	0.94	1.4	1.5	0.92	111	17	N/A
27B	0.94	1.4	1.5	1.1	93	23	2.81
31	0.94	1.4	1.5	1.3	90	23	2.93
35D	0.94	2.8	3.0	1.3	110	19	2.84
40	0.94	2.0	2.2	1.2	94	22	2.86
41	0.94	2.0	2.2	1.2	85	23	3.01

Table III. Powder Surface Atom Fractions*

XPS Peak	Powder Run No.	Glovebox Storage	Air Storage
C(1s)	40	-	0.64
	41	0.63	-
	24	0.60	0.62
O(1s)	40	-	0.04
	41	0.01	-
	24	0.03	0.06
Si(2p)	40	-	0.32
	41	0.36	-
	24	0.37	0.32

*Surface atom fraction determined using the integrated peak areas divided by their XPS sensitivity factors.

FIGURE CAPTIONS

Figure 1 -- Schematic of thermal plasma reactor used to prepare SiC powders.

Figure 2 -- XPS spectra showing C(1s) peaks for silicon carbide powders 40 and 24 after air storage. Carbide and C-C species are indicated by arrows.

Figure 3 -- XPS spectra showing Si(2p) peak for silicon carbide powders 40 and 24 after air storage. Difference spectrum was found relative to powder 40. Binding energies for some Si species are indicated by arrows.

Figure 4 -- Silicon-rich SiC powder 24, dispersed on carbon support film. The individual powder particles averaged 20 nm diameter, but are collected into large, irregular agglomerates. Free elemental carbon (see arrow) is present even in silicon-rich powders.

Figure 5 -- Selected area electron diffraction from Si-rich powder 24, showing composite Si plus beta-SiC rings.

Figure 6 -- High resolution image of Si-rich powder 24, showing Si, SiC, and amorphous C phases. Note that the agglomerate imaged is heavily sintered (i.e., "hard").

Figure 7 -- High resolution image of C-rich powder 40, showing elemental carbon both as discrete inclusions and as a thin film coating the SiC particles.

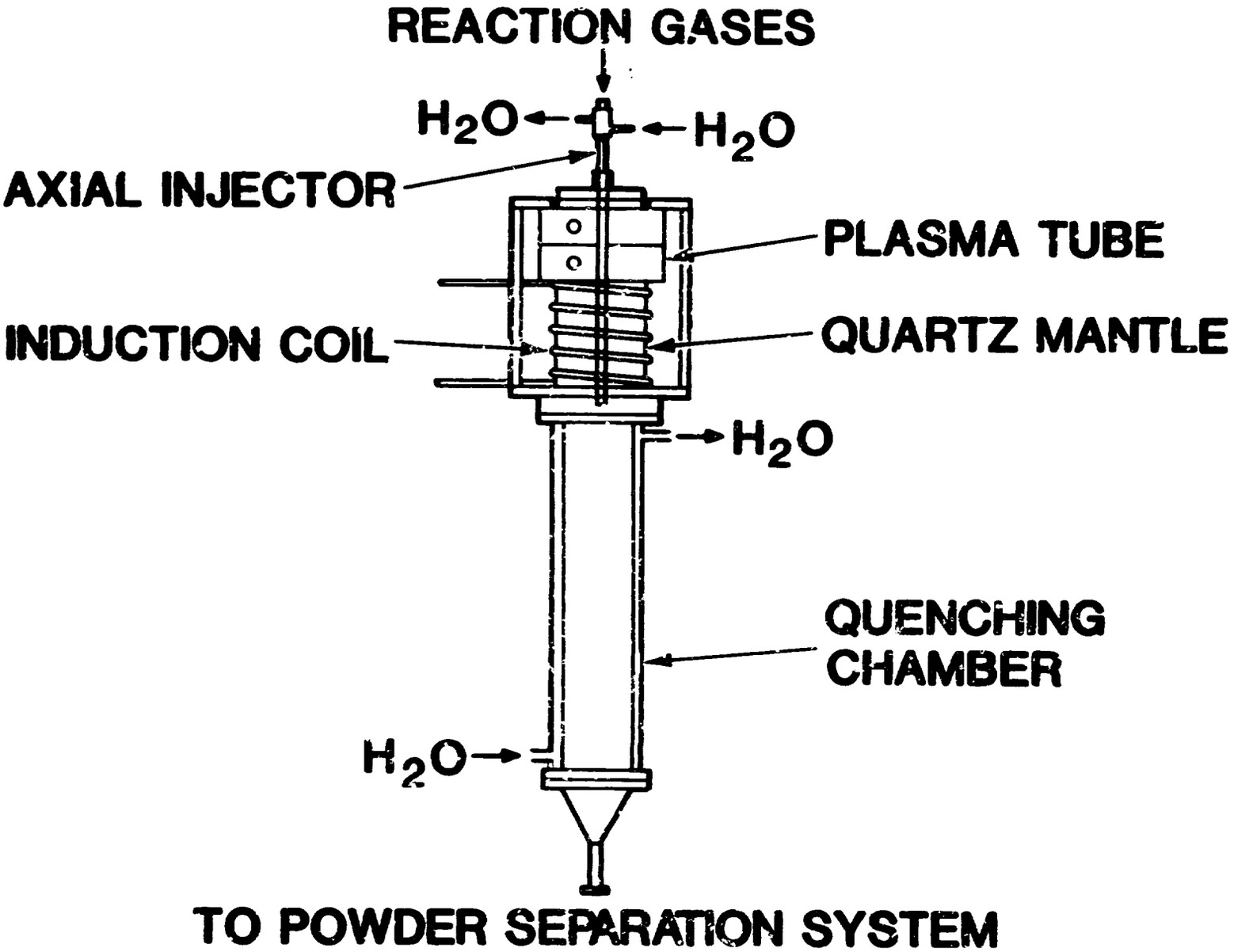
REACTION GASES
H_2O
H_2O
AXIAL INJECTOR
PLASMA TUBE
INDUCTION COIL
QUARTZ MANTLE
H_2O
QUENCHING CHAMBER
H_2O
TO POWDER SEPARATION SYSTEM

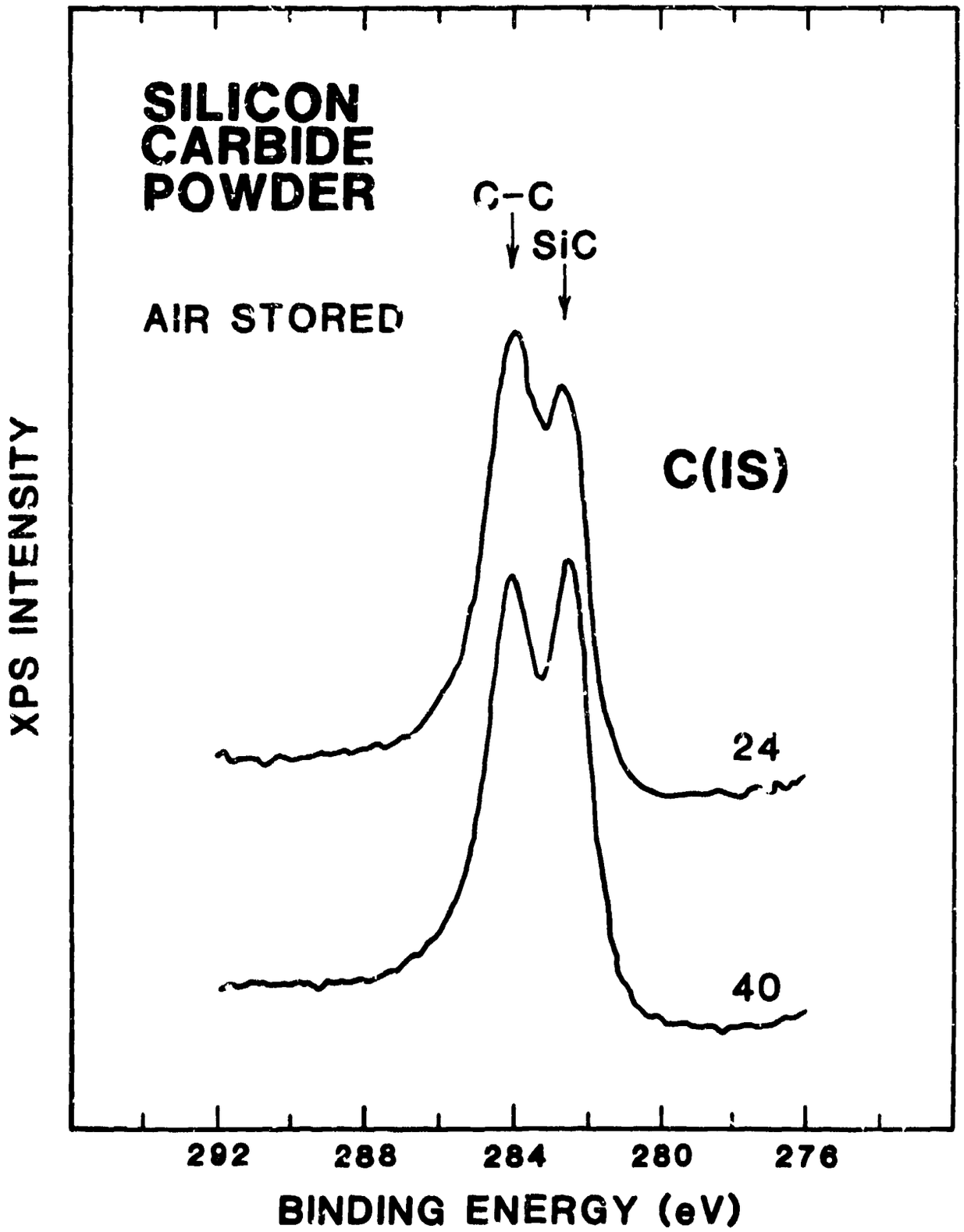
SILICON
CARBIDE
POWDER
C-C
SiC
AIR STORED
C(IS)
24
40
XPS INTENSITY
292
288
284
280
276
BINDING ENERGY (eV)

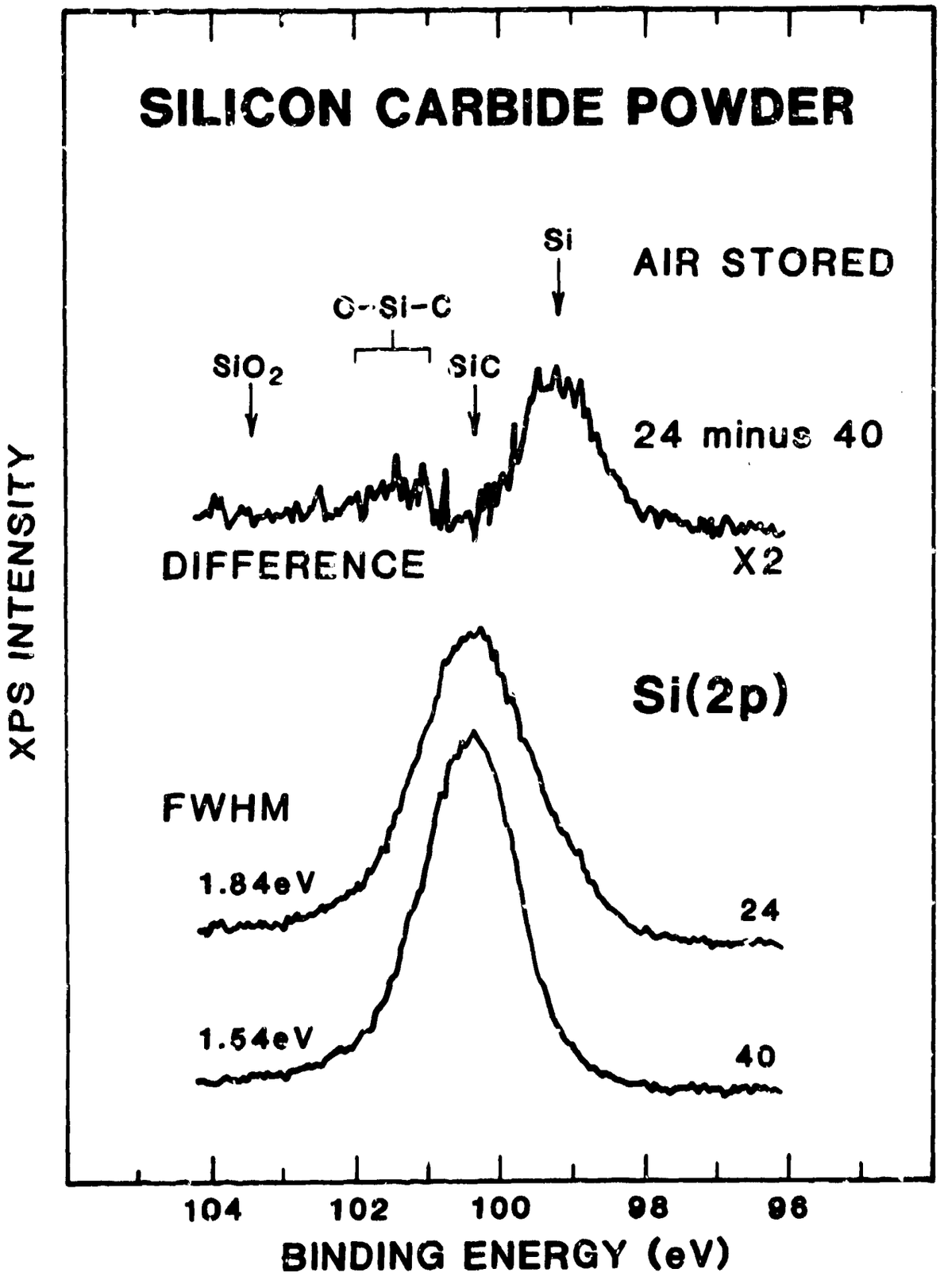
SILICON CARBIDE POWDER
Si
AIR STORED
C-Si-C
SiO2
SiC
24 minus 40
DIFFERENCE
X2
Si(2p)
FWHM
1.84eV
24
1.54eV
40
XPS INTENSITY
104
102
100
98
96
BINDING ENERGY (eV)


SIC Z
SI R.
SIC
SI
311
220
220
111
111